Enormous Surface-Enhanced Raman Scattering from Dimers of Flower-Like Silver Mesoparticles

*Hongyan Liang, Zhipeng Li, Zhuoxian Wang, Wenzhong Wang, Federico Rosei, Dongling Ma, and Hongxing Xu**

Surface-enhanced Raman scattering (SERS) spectroscopy is a powerful and extremely sensitive spectroscopic tool that can provide a spectral fingerprint of molecules.[1–4] In SERS, the small Raman cross-section of molecules is dramatically enhanced by several orders of magnitude due to the huge electromagnetic (EM) field enhancement caused by the excitation of plasmons on the surfaces of metals.[5–8] In nanostructures with two or more particles, sub-10 nm gaps will give rise to interparticle interaction that produces a significant change of optical response and enormous enhancement of the EM field. The coupling effect between two adjacent metal structures creates an efficient "hot spot" for SERS. As previously reported, the SERS enhancement factor (EF) in silver particle dimers is up to 10^{10}, which is sufficient for single molecules detection.[9,10] Various nanostructures containing nanogaps have been developed for SERS substrates, such as nanohole or nanoparticle arrays,[11,12] hole–particle pairs,[13] nanocube dimers,[14] nanoparticle-nanowire couples,[15] nanorod dimers,[16] etc. Both experimental and theoretical studies have proven that the nanostructures' shape, size, topography, arrangement, and the interparticle distance greatly affect the coupling effect.[17–22] For example, for individual nanoparticles with the diameter smaller than 50 nm, only a dipolar plasmon mode can be excited. When particle size further increases, higher-order multipolar plasmonic modes begin to appear[23,24] and the absorption peak corresponding with the interparticle interaction in the visible range decreases due to the red-shift of surface plasmon resonance. Structures with smooth surface behave quite differently from those with rough surface. For spherical Au or Ag nanoparticles with smooth surfaces, the plasmon band is narrow and falls within the visible range. However, surface roughness of only several nanometers is sufficient to result in the red shift of surface plasmon modes.[25,26] In addition, the protrusions on the rough surface of two adjacent particles will increase the possibility of forming multiple hot spots in one single dimer. Both the size and the surface topography influence SERS enhancement significantly. As reported before, single mesoparticles with roughened morphology could generate SERS EF more than 10^7 with good reproducibility,[27–29] which exceeds that obtained on single smooth nanoparticles by 3 or 4 orders of magnitude.

In this paper, we report an ≈10 to 100 times higher SERS enhancement of flower-like silver mesoparticle dimers compared to single mesoparticles. As the flower-like silver mesoparticles are about one micrometer in diameter, it is possible to move them under a conventional optical microscope with a micro-manipulator. The incident-polarization-dependent SERS of the particle dimers under spatial management clearly shows that the interparticle coupling results in additional one or two orders of enhancement over individual particles. Moreover, we found the nanogaps in dimers formed in this controlled way have better SERS performance than randomly assembled dimers, which may offer a low-cost and simple method to controllably form dimers for SERS applications.

Flower-like silver mesoparticles were obtained by reducing $AgNO_3$ with ascorbic acid in aqueous solution.[28] To compare the enhancement of the SERS signals between individual particles and dimers, malachite green isothiocyanate (MGITC) is employed as probe molecules. MGITC can bind strongly to the silver surface by the sulfur atom of its isothiocyanate group, and the absorption peak of MGITC is near the excitation laser wavelength at 632.8 nm used here, thus additional resonance Raman enhancement can be expected. An upright microscope was used to excite and collect the Raman signal. As reported before, owing to the micrometer scale size, the individual mesoparticles could be observed clearly under a 50× or 100× objective,[28] therefore, it is possible to distinguish the individual particles and

Dr. H. Y. Liang, Prof. F. Rosei, Prof. D. Ma
Institut National de la Recherche Scientifique
University of Quebec
1650 Boulevard Lionel-Boulet
Varennes, Québec, J3X 1S2, Canada
Prof. Z. P. Li
Beijing Key Laboratory of Nano-Photonics and Nano-Structure (NPNS)
Department of Physics
Capital Normal University
Beijing, 100048, China
Dr. Z. X. Wang, Prof. H. X. Xu
Institute of Physics
Chinese Academy of Science
Beijing, 100190 China
E-mail: hongxingxu@aphy.iphy.ac.cn
Prof. W. Z. Wang
School of Science
Minzu University of China
Beijing, 100081 China

DOI: 10.1002/smll.201201081

NANO MICRO small

dimers. By marking the samples with an indexed transmission electron microscopy (TEM) grid, the same object identified in optical images could be investigated later by scanning electron microscopy (SEM) imaging for the detailed topography. A half-wave plate inserted into the optical route was used to systematically rotate the plane of polarization of the incident laser. Therefore, incident polarization dependent SERS measurements could be detected. Raman spectra were collected by a Renishaw inVia micro-Raman spectroscopy system. All these measurements were preformed under exactly same experimental conditions. **Figure 1**A,C show the typical Raman spectra of the individual particles and dimers. The corresponding SEM images are shown in Figure 1B,D, respectively. These spectra show the main vibrational features of MGITC molecules with the Raman shift at 1173, 1365, and 1615 cm^{-1}. The intensities of these peaks obtained from MGITC molecules on the coupled dimers are usually ≈10 to 100 times larger than those on the individual particles, based on the measurement of dozens of examples (Figure S1, Supporting Information). Even considering that the dimer accommodates twice as many molecules as the individual particle, there still is a giant additional SERS enhancement, which is expected as a result of the coupled gaps formed between two mesoparticles. To confirm the coupling effect, incident polarization dependent SERS measurements of a dimer were carried out. As shown in Figure 1E, when the polarized excitation mode is parallel to the dimer axis, the SERS enhancement reaches maximum. The apparent incident polarization dependence indicates the SERS enhancement could be contributed by the coupling at the junction of the dimer, which is similar to the case of smooth spheres.[9,18]

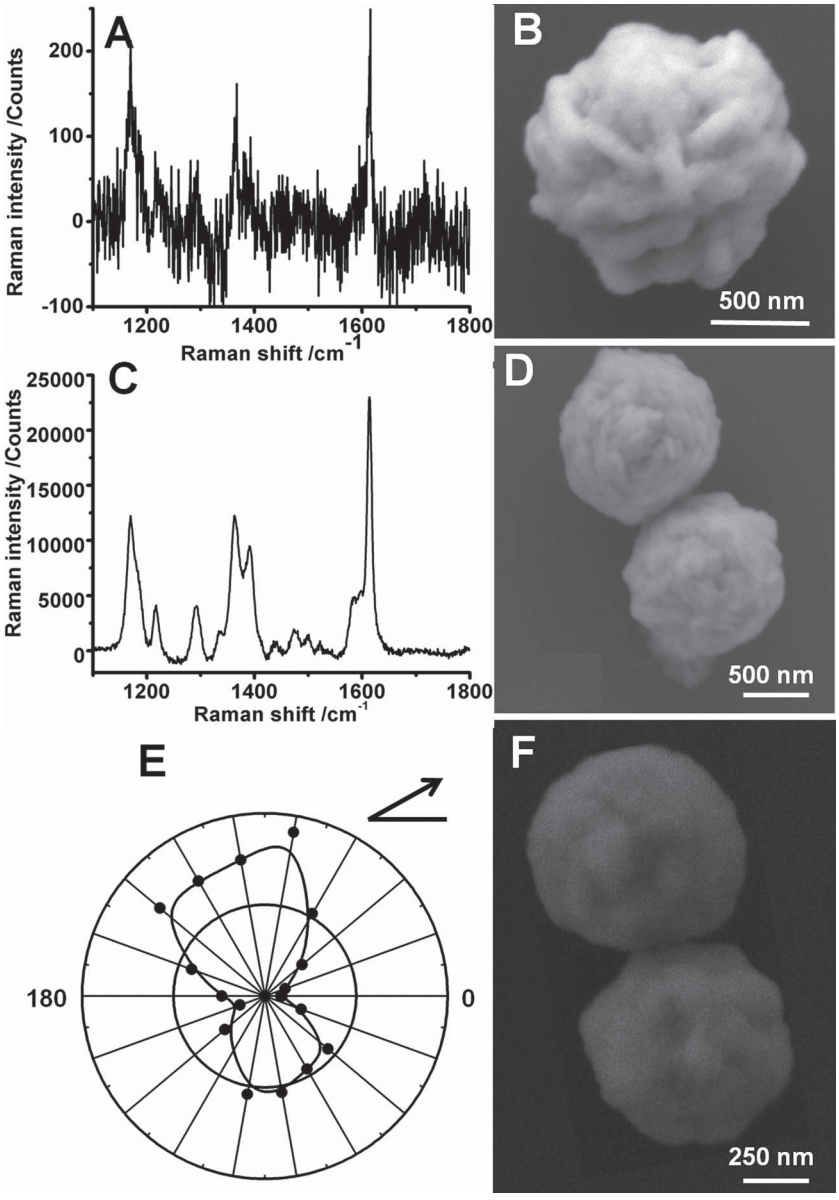

Figure 1. A) SERS spectrum of MGITC detected from an individual flower-like mesoparticle and B) its corresponding SEM image. C) SERS spectrum of MGITC detected from a dimer and D) its corresponding SEM image. E) Polar plots of the Raman peak intensities of 1615 cm^{-1} detected from a dimer and F) its corresponding SEM image, showing that the rotation angle of the dimer axis is ≈120° with respect to a horizontal line.

To study the physical mechanism in the case of flower-like silver mesoparticle dimer, Raman imaging that can show the spatial distribution of SERS enhancement over the whole surface was used to provide a more fundamental understanding of such an additional SERS enhancement. The Raman shift of 1615 cm^{-1} was chosen for imaging measurement. It is worth pointing out that the dimers in Figure 1D,F were obtained by self-assembly. A common problem with self-assembled dimers is ill-controlled configurations. To better investigate the coupling effect, it is highly desirable to be able to control the formation of the dimers. We have achieved this by using a micro-manipulator to move the individual particles under an optical microscope. In this way, high SERS active dimers can be formed or broken for studying SERS in situ. Compared to conventional nano-manipulation with atomic force microscopy (AFM), which only works for nanoscale particles, the micro-manipulator provides the capability to manipulate larger individual mesoparticles with diameter ranging from several hundred nanometers to micrometers. Although it requires patience and carefulness to manipulate the object under visual guidance and simultaneous imaging, if properly done, this technique enables one to assemble mesoparticles with well-controlled geometry for individual structure investigations. Such an approach does not require tedious sample preparation procedures and breaks the limitation on the types of samples that can be studied. Since the gap distance between the manipulated metal particles is limited by the coating ligands on the particles, with a proper push by the

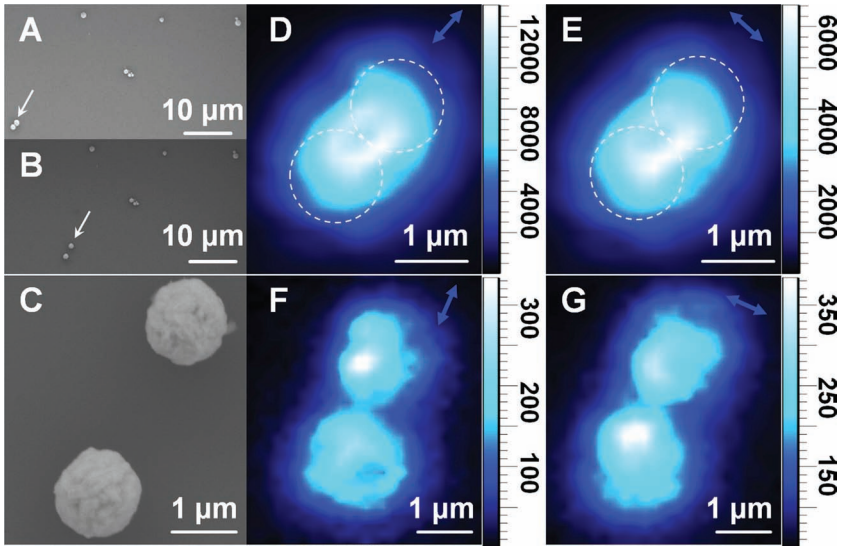

Figure 2. A) SEM image of a self-assembled dimer marked by an arrow. Corresponding Raman images at parallel (D) and perpendicular (E) incident polarization with respect to the dimer axis. The white circles represent the location of flower-like mesoparticles. B) SEM and C) high-magnification SEM images of two individual flower-like mesoparticles after being separated from the dimer via micro-manipulation. Corresponding Raman images at parallel (F) and perpendicular (G) incident polarization with respect to the symmetric axis of detected flower-like mesoparticles. The blue arrows show the polarization of incident laser light.

micro-manipulator, it is easy to achieve the minimum gap size, i.e., twice of ligand length, for maximum SERS enhancement. Thus the new method not only greatly reduces the manipulation time and increases the success rate of long-range manipulation, but also easily pushes the SERS enhancement to the maximum limit of the manipulated dimers. It is necessary to point out that movement of the micro-manipulator is artificial controlled so the gap distance is mainly determined by the thickness of ligands on particle's surface, which was monolayer in general. The SEM image of a self-assembled dimer is marked by an arrow in **Figure 2**A. Corresponding Raman images under parallel and perpendicular incident polarization directions (as indicated by blue arrows) with respect to the dimer axis are shown in Figure 2D,E. The Raman intensities and spatial distribution are indicated by the color and shape of the bright spots, respectively. The maximum intensity at the parallel direction is nearly twice that at the perpendicularly polarized direction. The reason that the SERS enhancement at the perpendicular incidence does not completely vanish is the formation of multiple gaps with randomly oriented directions by protrusions on roughened particle surfaces. We then used the micro-manipulator to separate the dimer about 2 μm into two individual particles as marked in Figure 2B and the high-magnification SEM image is shown in Figure 2C. Corresponding SERS images are shown in Figure 2F,G with the incident polarization indicated by blue arrows. The maximum SERS intensities are one order of magnitude lower than those from the dimer before the micro-manipulation. These results indicate that the 2 μm separation is enough to reduce the interparticle coupling between two nearby particles. The SERS enhancements of the individual flower-like silver mesoparticles are dominated by the surface roughness rather than the interparticle coupling effect. These results totally support the assumption that the additional SERS enhancement observed in the dimer is primarily contributed by the interparticle interaction.

In another scenario, we studied the SERS of two initially isolated flower-like silver mesoparticles (marked by an arrow in **Figure 3**A) and their dimer (Figure 3B,C) were formed by mico-manipulation. The Raman images of these two individual particles are shown in Figure 3D–F with the incident polarization indicated by blue arrows. Obviously, there is no incident polarization dependence for the single particles. The coupling between these two particles can be neglected. As the original location of the upper particle is much closer to the laser spot center, the upper spot in the Raman images is brighter. Then the upper one is pushed by the micro-manipulator towards the lower one to form a dimer. Based on the SEM images of the dimer shown in Figure 3B,C, the dimer has a sub-5 nm gap located at the junction between two particles. When the incident light is parallel to the axis of the dimer as shown in Figure 3G, the maximum SERS intensity located around the dimer junction is 10 times higher than that on individual particles. When the incident polarization is tuned to 45° angle, the maximum SERS intensity decreases. At the same time, the hot spot at the junction shrinks. When the incident polarization is perpendicular to the dimer axis, the hot spot at the junction disappears, and two separate bright spots located at the center of each particle appear instead. The SERS intensity under the perpendicular excitation is nearly 10 times lower than that under the parallel polarized incidence, as in this case the enhancement is solely contributed by the surface roughness.[28] Both the decrease of the SERS intensity and the change of the hot spot under perpendicular excitation provide a direct proof for the coupling effect in this dimer. In addition, the mechanical micro-manipulation of micrometer-sized, flower-like silver particles enables the easy formation of a high quality dimer with a large hot spot area. The micro-manipulation method greatly improves the yield of dimers with high Raman activities.

Because the size of flower-like mesoparticle is much larger than the incident laser wavelength, the EM coupling between two flower-like mesoparticles is dominated by multipoles couplings. To evaluate this enhancement effect, we applied the generalized Mie calculation[30] for two silver mesospheres. The silver sphere diameter used in our calculation was set to be 1 μm, and the gap distance between two particles is estimated to be 3 nm by accounting the coverage of ascorbic acid and MGITC molecules. The multipoles are taken up to 50, which is enough for the convergence of the simulation. Under the excitation of 633 nm, the EM field distributions of the dimer at two orthogonal incident polarizations are shown in **Figure 4**. The maximum EM field enhancement in the gap region is about 27 times (corresponding to SERS

small NANO MICRO

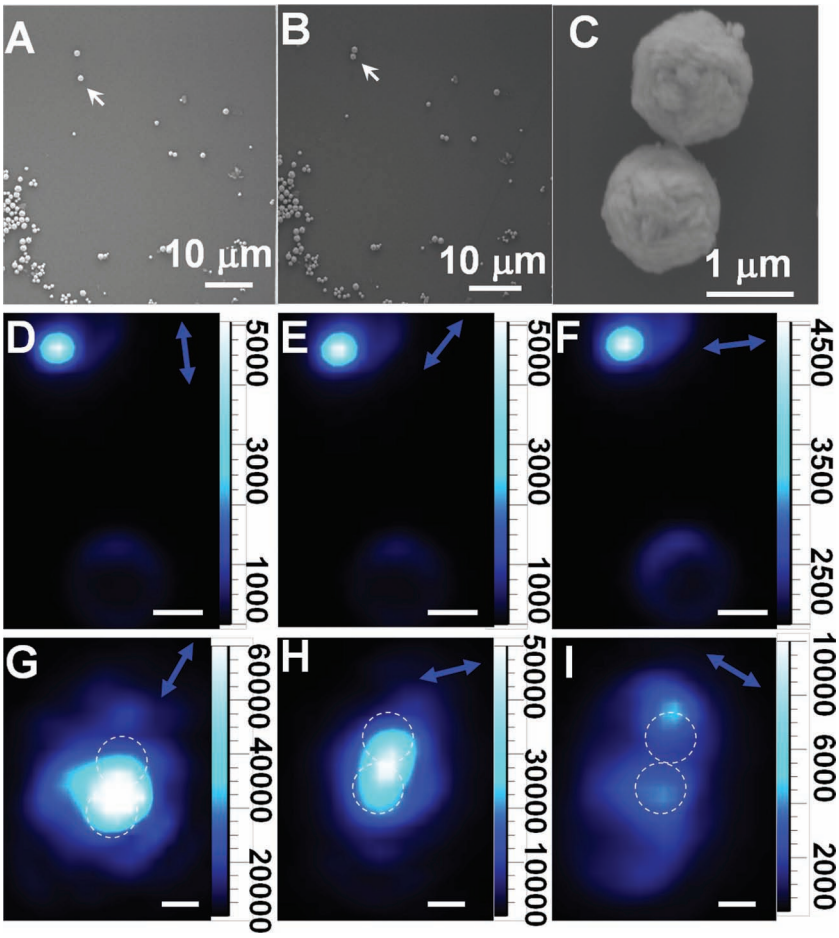

Figure 3. A) SEM image of two isolated flower-like mesoparticles marked by an arrow. Corresponding Raman images at parallel (D), 45° angle (E), and perpendicular (F) incident polarization with respect to the symmetric axis of detected particles. B) SEM and C) high magnification SEM image of the dimer formed by manipulating two individual flower-like mesoparticles in (A). Corresponding Raman images at parallel (G), 45° angle (H), and perpendicular (I) incident polarization with respect to the dimer axis. The white circles represent the location of the flower-like mesoparticles. The blue arrows show the polarization of incident laser light. The scale bars in (D–I) are 1 μm.

enhancement about 5×10^5) larger than the incident light, when the excitation is parallel to the dimer axis as shown in Figure 4A,B. When the incident light is perpendicular to the dimer axis as shown in Figure 4C,D, the SERS enhancement is only two-fold in the side of the dimer due to the weak coupling between spheres.

Compared with the experiment results, the surface roughness of flower-like rough particles gives the main contribution to their SERS,[28] which is different from that of smooth spheres. The calculation result for a single smooth sphere is shown in Figure S3 (Supporting Information). We also synthesized nearly smooth, quasi-spherical mesoparticles which have the similar size with the flower-like mesoparticles and experiment results are shown in Figure S1,S4 (Supporting Information). The gap-distance between two quasi-spherical mesoparticles is supposed to be similar as in the flower-like particles case. However, for the rough particle dimer, the SERS is dominated by the interparticle coupling and is highly dependent on incident polarization. This is qualitatively consistent with the above simulations based on the generalized Mie theory.[30] It is worthwhile to note that, theoretically, in the dimer of two perfect smooth spheres, the maximum SERS enhanced volume is highly confined in the center of the junction, as shown in Figure 4A,B, and the size of the hot spot is less than 100 nm. While, for the rough mesoparticle dimers, the size of hot spot shown in Figure 3G and Figure S5 (Supporting Information) is larger than 1.5 μm, as indicated by the brightest color (the resolution of Raman image is about 500 nm according to Abbe's formula), which is much larger than that in the smooth sphere dimer case. As the matter of fact, the nearly-smooth mesoparticle dimers show the size of hot spot around 500 nm in diameter, as shown in Figure S2 (Supporting Information). In view of the fact that the surface of mesopartices is not absolutely smooth and the spherical shape is not perfect either, the size of the hot-spot area (500 nm in diameter) is considered consistent with the theoretically calculated value. The large area of hot spot of flower-like mesoparticle dimers is due to the formation of multiple gaps at the junction of dimer by protrusions or dimples on roughened particle surfaces. Such large area of the hot spot easily formed in the current study could be beneficial to SERS applications.

Since the gap sizes in self-assembly dimers are randomly in the range of several to tens of nanometers, which are hardly distinguished under an optical microscope when Raman measurements are performing, it is worth to point out that most dimers formed by self-assembly display no obvious coupling effect. It is simply due to that large gaps could reduce the coupling effect significantly and make the dimer SERS inactive to the incident polarization, although the basic enhancement of individual roughed particles still exists. By the micro-manipulation on flower-like roughed particles, dimers are easily formed with the total SERS EF estimated to be above 10^8, whereas it is about 10^7 for single flower-like particles. We have studied dozens of dimers formed by micro-manipulation, except the one shown in Figure 3, another typical one is shown in Figure S5 (Supporting Information).

In conclusion, SERS on flower-like silver mesoparticle dimers by means of the micro-manipulation is performed. The measured SERS enhancements are found to be ≈10 To 100 times higher on dimers than that on individual mesoparticles. The observation of highly dependence of incident polarization illustrates that, even though the surface roughness is dominant for SERS on the individual mesoparticles with rough surface topography, the coupling effect

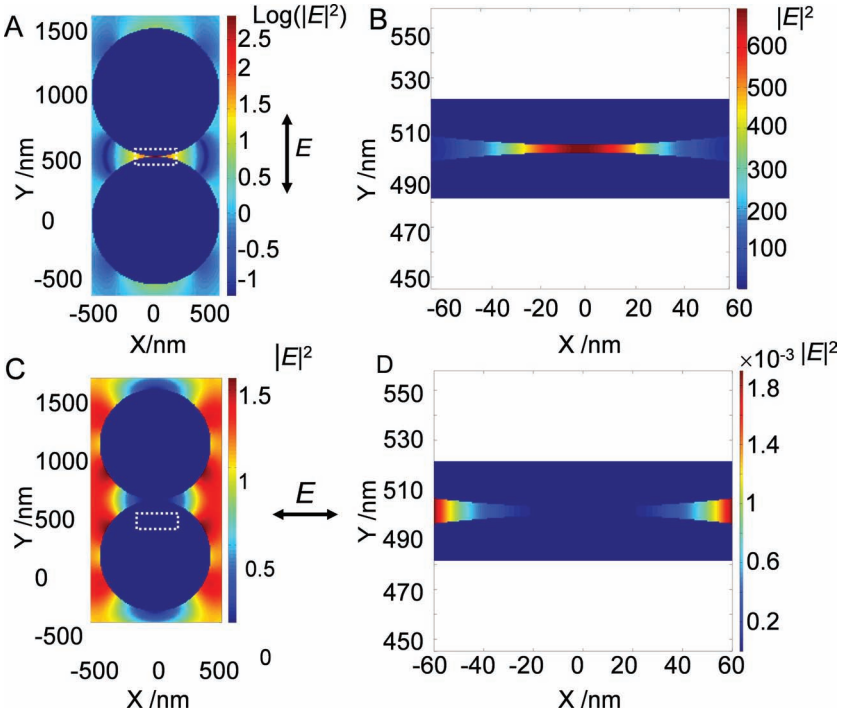

Figure 4. Theoretical calculation of the optical intensity (E^2) distribution around silver sphere dimer with the diameter of 1 μm and interparticle distance of 3 nm. The incident wavelength is 633 nm. A) The excitation polarization is parallel to the dimer axis and B) the enlarged image of the center in (A), as indicated by a white rectangle. C) The excitation polarization is perpendicular to the dimer axis and D) the enlarged image of the center in (C), as indicated by a white rectangle.

still gives a significant additional SERS enhancement in their dimers. In addition, the use of the micro-manipulation allows us to achieve dimers with high SERS enhancement controllably and reproducibly. This work contributes to the understanding the SERS enhancement mechanism in the roughened mesoparticles dimer system, as well as to controllably realizing SERS substrates with large hot spot area for high enhancement.

Experimental Section

The flower-like silver mesoparticles are obtained by reducing $AgNO_3$ with ascorbic acid under the protection of capping agent. In a typical synthesis, a $AgNO_3$ aqueous solution (0.3 mL, 1 M) and a poly(vinyl pyrrolidone) (PVP, Mw ≈ 40 000, 2 mL, 0.1 M) aqueous solution were added to deionized water (10 mL) in a beaker with a magnetic stirrer at room temperature. The concentration of PVP was calculated in terms of the repeating units. An ascorbic acid (0.2 mL, 1 M) aqueous solution was then quickly injected into the vigorously stirred mixture. The solution became grey immediately and then changed to dark grey a few minutes later, which indicated the appearance of a large quantity of colloidal silver particles. By this procedure, colloidal silver flowers with a radius of about 1 μm could be obtained. The nearly smooth, quasi-spherical silver mesoparticles were synthesized via a similar process, with the modification of the quantity of $AgNO_3$, ascorbic acid and PVP to (0.05 mL, 1 M), (0.04 mL, 1 M), (0.05 mL, 0.1 M), respectively and the additional introduction of a HNO_3 aqueous solution (0.05 mL, 15 M). A sample of the silver particles was obtained by centrifugation and was washed with ethanol several times to remove the excess surfactant.

Samples for SERS measurements were prepared by the following processes: MGITC molecules solution (0.1 mL, 10^{-6} M) was mixed with the same volume of silver suspension. The corresponding concentration of the silver mesoparticles in the suspension was estimated to be about 10^{-12} M and this means that there were of the order of 10^6 MGITC molecules per silver particle. The high density of MGITC solution could ensure that there are some molecules reside in the junctions between two particles. The mixed solution was allowed to incubate overnight to achieve a high adsorption of MGITC molecules on the surface of particles. The excess of free MGITC molecules in the supernatant after centrifugation at 3000 rpm for 3 min were removed. The precipitate was redispersed in ethanol. Through this process, monolayer of MGITC molecules are left on the surface of the particles, however, multilayers also possible exist, especial on the surface of crevices. By comparing the absorbance of MGITC molecules in the solution before added Ag particles and in the supernatant after centrifugation to remove Ag particles, eighty percent of the molecules are estimated to adsorb onto the silver particle. Further, one drop of the solution containing silver particles was spin-coated on a clean Si slide, and then rinsed with ethanol to remove unabsorbed particles and dried under a stream of nitrogen. After adsorbing particles, the Si slide was decorated with an indexed TEM grid consisting of 100 μm × 100 μm grids, which facilitated post situ both the optical and SEM imaging of desired particles. All experiments were performed on air-Si interfaces.

The Raman signal was measured with a Renishaw inVia micro-Raman spectroscopy system. Raman excitation was performed with a 632.8 nm HeNe laser at low power (in the μW range under the objective) to minimize heating and photochemical effects. The laser was blocked by a 633 nm edge filter. Incident polarization was tuned by a half wave plate in order to effectively excite randomly oriented dimers. The sample was mounted on an XY stage of a Leica microscope, equipped with a 100× (NA = 0.95) objective, which was used for excitation and collection, and the spot size was around 1 μm in diameter. The measurement of the Raman image was performed using the TE air cooled 576 × 400 charge coupled detector (CCD) array in a confocal Raman system with a spectroscopic window width of ±20 cm^{-1}, while the unfocused laser light spread all over the measure area. The Raman spectra were collected in the backscattering geometry by the same CCD.

A micromanipulator (MMO-202ND, Narishige) equipped on an optical microscope was used to manipulate the particles in 3-dimension. It could form or break the dimers controllably without damaging the particles.

NANO MICRO small

Supporting Information

Supporting Information is available from the Wiley Online Library or from the author.

Acknowledgements

H.Y.L. and Z.P.L. contributed equally to this work. This work was supported by MOST Grant (2009CB930700), NSFC Grants (Nos.10625418, 10874233, 10904171, 11004237 and 11134013), the "Knowledge Innovation Project" (KJCX2-EW-W04) of CAS, Beijing Nova Program (2011079), Beijing Natural Science Foundation (Grant Nos. 1122012) and Financial support from the Merit Scholarship Program for Foreign Students from the Ministère de l'Éducation, du Loisir et du Sport du Québec.

[1] A. Campion, P. Kambhampati, *Chem. Soc. Rev.* **1998**, *27*, 241.
[2] M. Moskovits, *Top. Appl. Phys.* **2006**, *103*, 1.
[3] M. Yang, R. Alvarez-Puebla, H. S. Kim, P. Aldeanueva-Potel, L. M. Liz-Marzán, N. A. Kotov, *Nano Lett.* **2010**, *10*, 4013.
[4] J. F. Li, Y. F. Huang, Y. Ding, Z. L. Yang, S. B. Li, X. S. Zhou, F. R. Fan, W. Zhang, Z. Y. Zhou, D. Y. Wu, B. Ren, Z. L. Wang, Z. Q. Tian, *Nature* **2010**, *464*, 392.
[5] N. A. Hatab, C. H. Hsueh, A. L. Gaddis, S. T. Retterer, J. H. Li, G. Eres, Z. Zhang, B. Gu, *Nano Lett.* **2010**, *10*, 4952.
[6] M. Schnell, A. Garcia-Etxarri, A. J. Huber, K. Crozier, J. Aizpurua, R. Hillenbrand, *Nat. Photonics* **2009**, *3*, 287.
[7] H. Cang, A. Labno, C. Lu, X. Yin, M. Liu, C. Gladden, Y. Liu, X. Zhang, *Nature* **2011**, *469*, 385.
[8] Z. P. Li, S. P. Zhang, N. J. Halas, P. Nordlander, H. X. Xu, *Small* **2011**, *7*, 593.
[9] H. X. Xu, E. J. Bjerneld, M. Käll, L. Börjesson, *Phys. Rev. Lett.* **1999**, *83*, 4357.
[10] A. M. Michaels, M. Nirmal, L. E. Brus, *J. Am. Chem. Soc.* **1999**, *121*, 9932.
[11] F. J. Garcia de Abajo, *Rev. Mod. Phys.* **2007**, *79*, 1267.
[12] F. Le, D. W. Brandl, Y. A. Urzhumov, H. Wang, J. Kundu, N. J. Halas, J. Aizpurua, P. Nordlander, *ACS Nano* **2008**, *2*, 707.
[13] H. Wei, U. Hakanson, Z. L. Yang, F. Hook, H. X. Xu, *Small* **2008**, *4*, 1296.
[14] S. Y. Lee, L. Hung, G. S. Lang, J. E. Cornett, I. D. Mayergoyz, O. Rabin, *ACS Nano* **2010**, *4*, 5763.
[15] H. Wei, F. Hao, Y. Z. Huang, W. Z. Wang, P. Nordlander, H. X. Xu, *Nano Lett.* **2008**, *8*, 2497.
[16] K. D. Alexander, K. Skinner, S. P. Zhang, H. Wei, R. Lopez, *Nano Lett.* **2010**, *10*, 4488.
[17] F. Svedberg, Z. P. Li, H. X. Xu, M. Käll, *Nano Lett.* **2006**, *12*, 2639.
[18] T. Shegai, Z. P. Li, T. Dadosh, Z. Y. Zhang, H. X. Xu, G. Haran, *Proc. Natl. Acad. Sci. USA* **2008**, *105*, 16448.
[19] M. Pelton, J. Aizpurua, G. W. Bryant, *Laser Photonics Rev.* **2008**, *2*, 136.
[20] E. Hao, G. C. Schatz, *J. Chem. Phys.* **2004**, *120*, 357.
[21] N. J. Halas, S. Lal, W. S. Chang, S. Link, P. Nordlander, *Chem. Rev.* **2011**, *111*, 3913.
[22] A. R. Tao, S. Habas, P. Yang, *Small* **2008**, *4*, 310.
[23] J. X. Fang, S. Y. Du, S. Lebedkin, Z. Y. Li, R. Kruk, M. Kappes, H. Hahn, *Nano Lett.* **2010**, *10*, 5006.
[24] J. Xu, L. Zhang, H. Gong, J. Homola, Q. Yu, *Small* **2011**, *7*, 371.
[25] J. Rodriguez-Fernandez, A. M. Funston, J. Perez-Juste, R. A. Alvarez-Puebla, L. M. Liz-Marzan, P. Mulvaney, *Phys. Chem. Chem. Phys.* **2009**, *11*, 5909.
[26] H. Wang, G. P. Goodrich, F. Tam, C. Oubre, P. Nordlander, N. J. Halas, *J. Phys. Chem. B* **2005**, *109*, 11083.
[27] H. Wang, N. J. Halas, *Adv. Mater.* **2008**, *20*, 820.
[28] H. Y. Liang, Z. P. Li, W. Z. Wang, Y. S. Wu, H. X. Xu, *Adv. Mater.* **2009**, *21*, 4614.
[29] A. Trügler, J. C. Tinguely, J. R. Krenn, A. Hohenau, U. Hohenester, *Phys. Rev. B* **2011**, *83*, 081412.
[30] a) H. X. Xu, *Phys. Lett. A* **2003**, *312*, 411; b) Z. P. Li, H. X. Xu, J. Quant, *Spectrosc. Radiat. Transfer* **2007**, *103*, 394.

Received: May 17, 2012
Revised: June 27, 2012
Published online: August 7, 2012

